Fujita et al., http://www.jcb.org/cgi/content/full/jcb.201012074/DC1

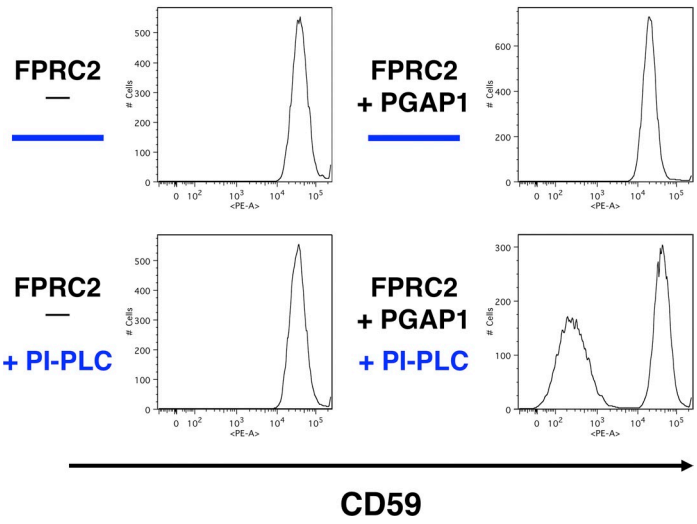

Figure S1. **Isolation of FPRC2 cells defective in PGAP1.** FPRC2 cells transiently transfected with an empty vector (FPRC2–) or PGAP1 containing plasmid (FPRC2 + PGAP1) were treated with or without PI-PLC at 37°C for 1 h. The cells were then stained with anti-CD59 antibody and PE-conjugated anti–mouse IgG, and analyzed by flow cytometry. CD59 was not cleaved by PI-PLC from the surface of FPRC2– cells, whereas the transfection of PGAP1 restored the sensitivity of CD59 to PI-PLC.

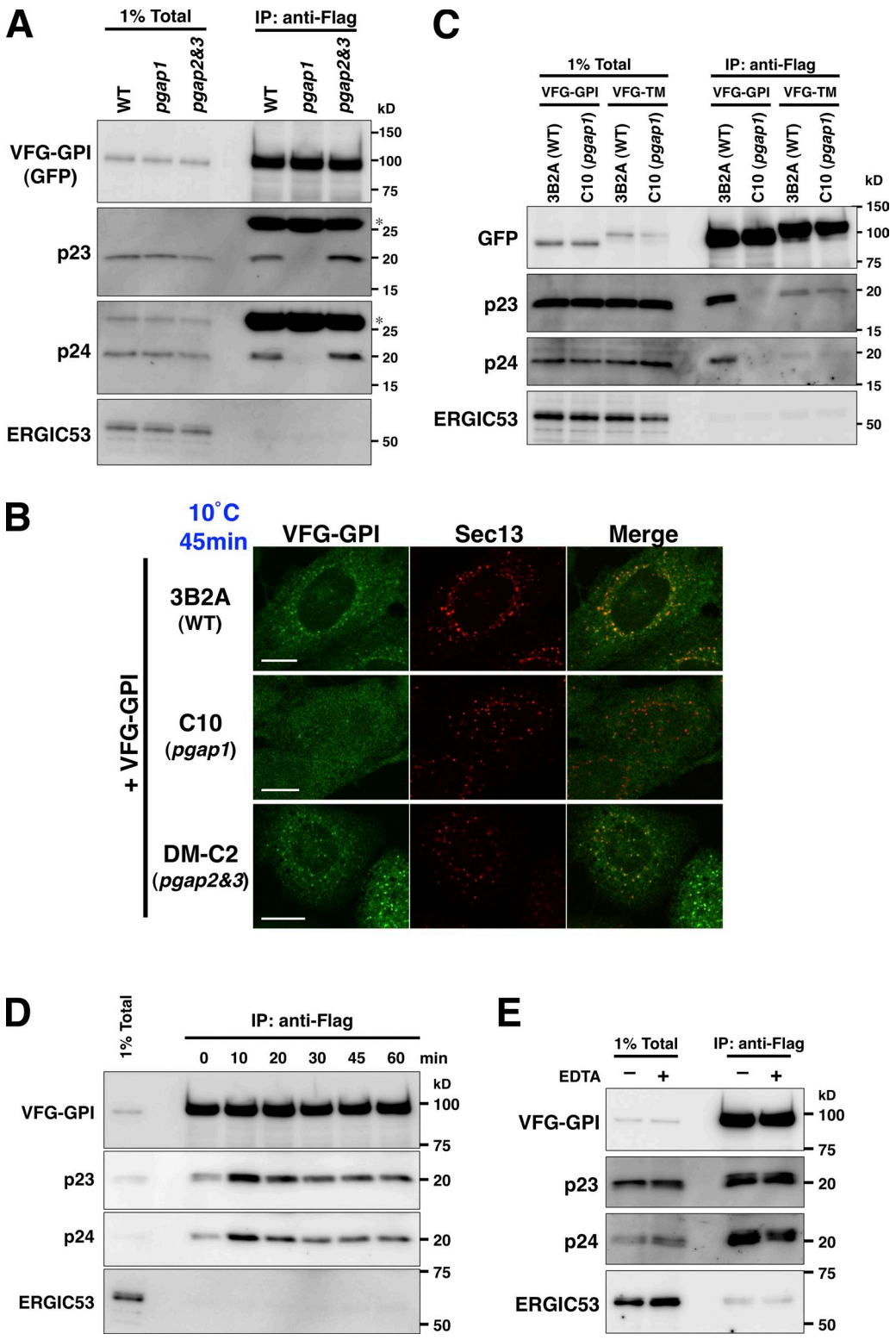

Figure S2. **Immunoprecipitation of VFG-GPI with p23 and p24.** (A) Immunoprecipitation of VFG-GPI with p23 and p24 in mutant cells defective in GPI fatty acid remodeling. 3B2A (WT), C10 (*pgap1* mutant), and DM-C2 (*pgap2&3* mutant) cells transiently transfected with VFG-GPI were incubated at 40°C for 24 h for ER accumulation of VFG-GPI and then at 32°C for 20 min to allow transport. After cell lysis, VFG-GPI was precipitated with anti-Flag beads, followed by immunoblotting. *, IgG light chains. (B) Sorting of GPI-APs into the ERES. VFG-GPI were transiently expressed in 3B2A (WT), C10 (*pgap1* mutant), and DM-C2 (*pgap2&3* mutant) cells and accumulated in the ER by incubating at 40°C for 24 h. After incubation at 10°C for 45 min, cells were fixed with 4% paraformaldehyde and stained with anti-Sec13 antibody to label the ERES. Bars, 10 µm. (C) Association of p23 and p24 with VFG-GPI was dependent on the GPI anchor. 3B2A (WT) and C10 (*pgap1*) cells transiently transfected with VFG-GPI or VFG-TM were incubated at 40°C for 24 h to accumulate the reporters at the ER, and incubated in complete medium at 32°C for 20 min. After cell lysis, VFG-GPI was precipitated with anti-Flag beads, followed by immunoblotting. (D) Time course of association of VFG-GPI with p23 and p24. FF8 cells were cultured with 1 µg/ml doxycycline at 40°C for 24 h to induce VFG-GPI expression and its accumulation in the ER. The cells were then incubated at 32°C for the indicated times, and kept on ice. After immunoprecipitation with anti-Flag beads, the precipitated proteins were analyzed by immunoblotting. (E) Metal dependency. FF8 cells were cultured with 1 µg/ml doxycycline at 40°C for 24 h, followed by incubation at 32°C for 20 min. The cells were lysed in lysis-IP buffer III with (+) or without (−) 5 mM EDTA, followed by immunoprecipitation. For washing, wash buffer III with (+) or without (−) EDTA was used. Precipitated proteins were analyzed by immunoblotting. In A, C, D, and E, an anti-p23, anti-p24, anti-ERGIC53, or anti-GFP antibody was used for immunoblotting, and total lysate corresponding to 1% and immunoprecipitates were used for analysis.

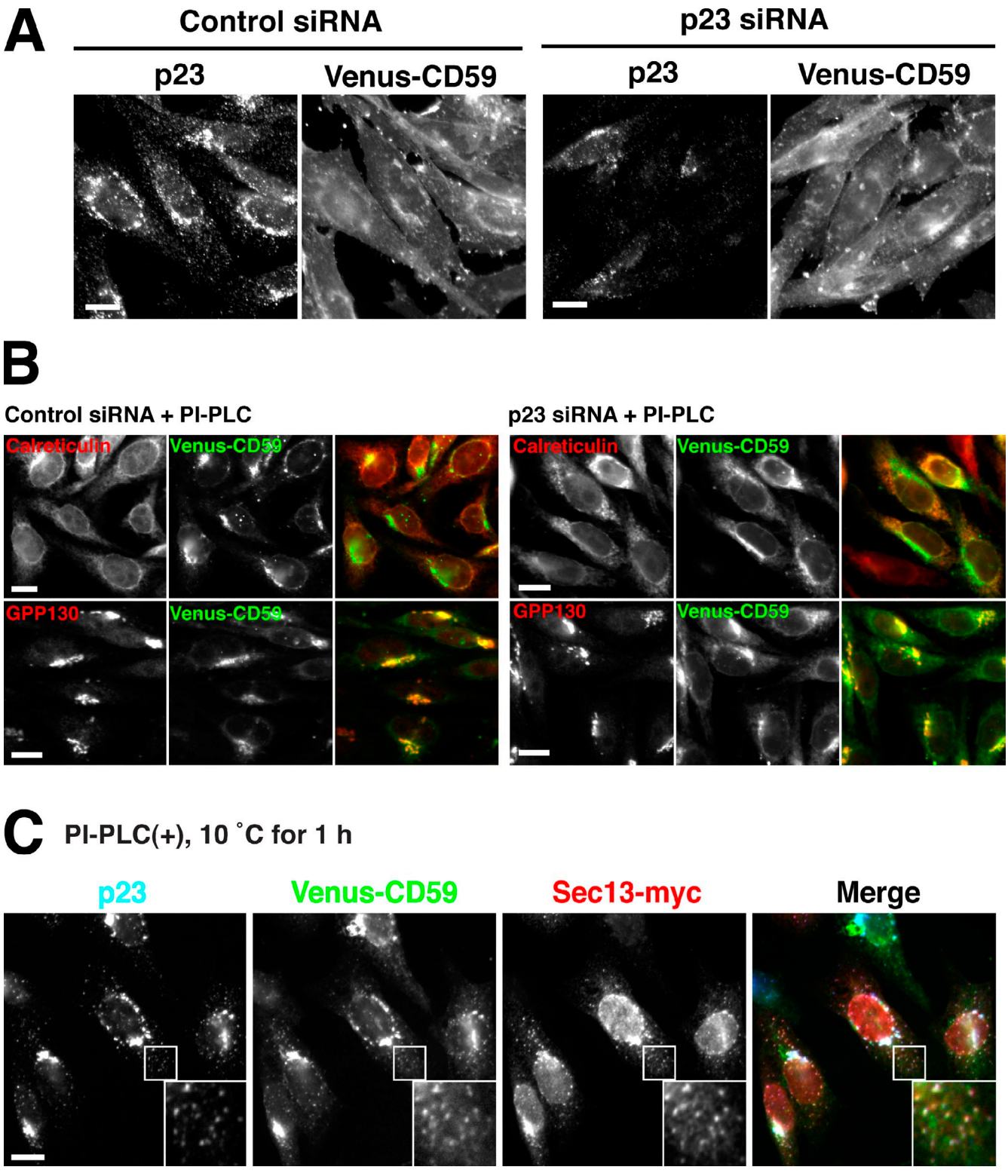

Figure S3. **Co-localization of Venus-CD59 with p23.** (A) Cell surface expression of Venus-CD59. CHO-K1 cells stably expressing Venus-CD59 were transfected with control RNA or siRNA against p23. After 72 h, the cells were fixed, followed by permeabilization, and immunostaining with anti-p23. Bars, 10 μm. (B) Intracellular localization of Venus-CD59 in p23 knockdown cells. CHO-K1 cells stably expressing Venus-CD59 were transfected with control RNA or siRNA against p23. After 72 h, the cells were treated with PI-PLC, fixed, and stained with anti-calreticulin or anti-GPP130 antibody. In the merged images, Venus-CD59 was shown in green and calreticulin or GPP130 was shown in red. Bars, 10 μm. (C) Co-localization of Venus-CD59 with p23 in the ERES. CHO-K1 cells stably expressing Venus-CD59 were transiently transfected with Sec13-myc, and the cells were treated with PI-PLC, incubated at 10°C for 1 h, fixed, and stained with anti-p23 antibody together with anti-myc antibody. In the merged images, p23, Venus-CD59, and Sec13-myc were shown in blue, green, and red, respectively. Boxed areas are enlarged in the bottom right. Bars, 10 μm.

>Tmed5 (p28)

1 MGVRMWLPFP MLLLSALPAT LLSGAAG**FTP SLDSDFTFTL PAGQKECFYQ**
51 **PMPLK**ASLEI EYQVLDGGEL DIDFHLASPE GRTLVFEQR**K SDGVHTVETE**
101 **DGDYMFCFDN TFSTISEK**VI FFELILDNMG EEVEGQEDWK KYITNTDVLE
151 MK**LEDILESI NSIK**SRLSKS GHIQTLLRAF EARDRNIQES NFDRVNFWSV
201 VNLMVMVVVS AIQVYTLKSL FEDKRKSRT

>Tmed9 (p25)

1 MRAFLLLLWL AARGSA**LYFH IGETEK**KC**FI EEIPDETMVI GNYR**TQLYDK
51 **QREEYQPATP GLGMFVEVKD PEDK**VILARQ YGSEGRFTFT SHTPGEHQIC
101 LHSNSTK**FSL FAGGMLR**VHL DIQVGEHAND YAEIAAK**DKL SELQLR**VRQ**L**
151 **VEQVEQIQK**E QNYQRWREER FRQTSESTNQ RVLWWSVLQT LILLAIGVCQ
201 MRHLKSFFEA KKLV

>Tmed2 (p24)

1 DVLVLLAALL ATASG**YFVSI DAHAEECFFE R**VTSGTKMGL IFEVAEGGFL
51 DIDVEITGPD NKGIYKGDRE SSGK**YTFAAH MDGTYK**FCFS NRMSTMTPK**I**
101 **VMFTIDIGEA PKGQDMETEA HQNKLEEMIN ELAVAMTAVK** HEQEYMEVRE
151 RIHRAINDNT NSRVVLWSFF EALVLVAMTL GQIYYLKRFF EVRRVV

>Tmed10 (p23)

1 MSGSSGPLSW PGPRPCALLF LLLLGPSSVL AISFHLPVNS RKCLREEIHK
51 **DLLVTGAYEI TDQSGGAGGL R**THLK**ITDSA GHILYAK**EDA TKGKFAFTTE
101 DYDMFEVCFE SKGTGR**IPDQ LVILDMK**HGV EAKNYEEIAK VEK**LKPLEVE**
151 **LRRLEDLSES IVNDFAYMK**K REEEMRDTNE STNTRVLYFS IFSMLCLIGL
201 ATWQVFYLRR FFKAKKLIE

Figure S4. **Identification of proteins associated with VFG-GPI in a pH-dependent manner.** Sequences of rat Tmed5 (p28), mouse Tmed9 (p25), Chinese hamster Tmed2 (p24), and golden hamster Tmed10 (p23). Protein bands at 25 kD and 20 kD in Fig. 8 B were digested with trypsin and analyzed by mass spectrometry. The fragments detected by MS/MS analysis are shown in red.

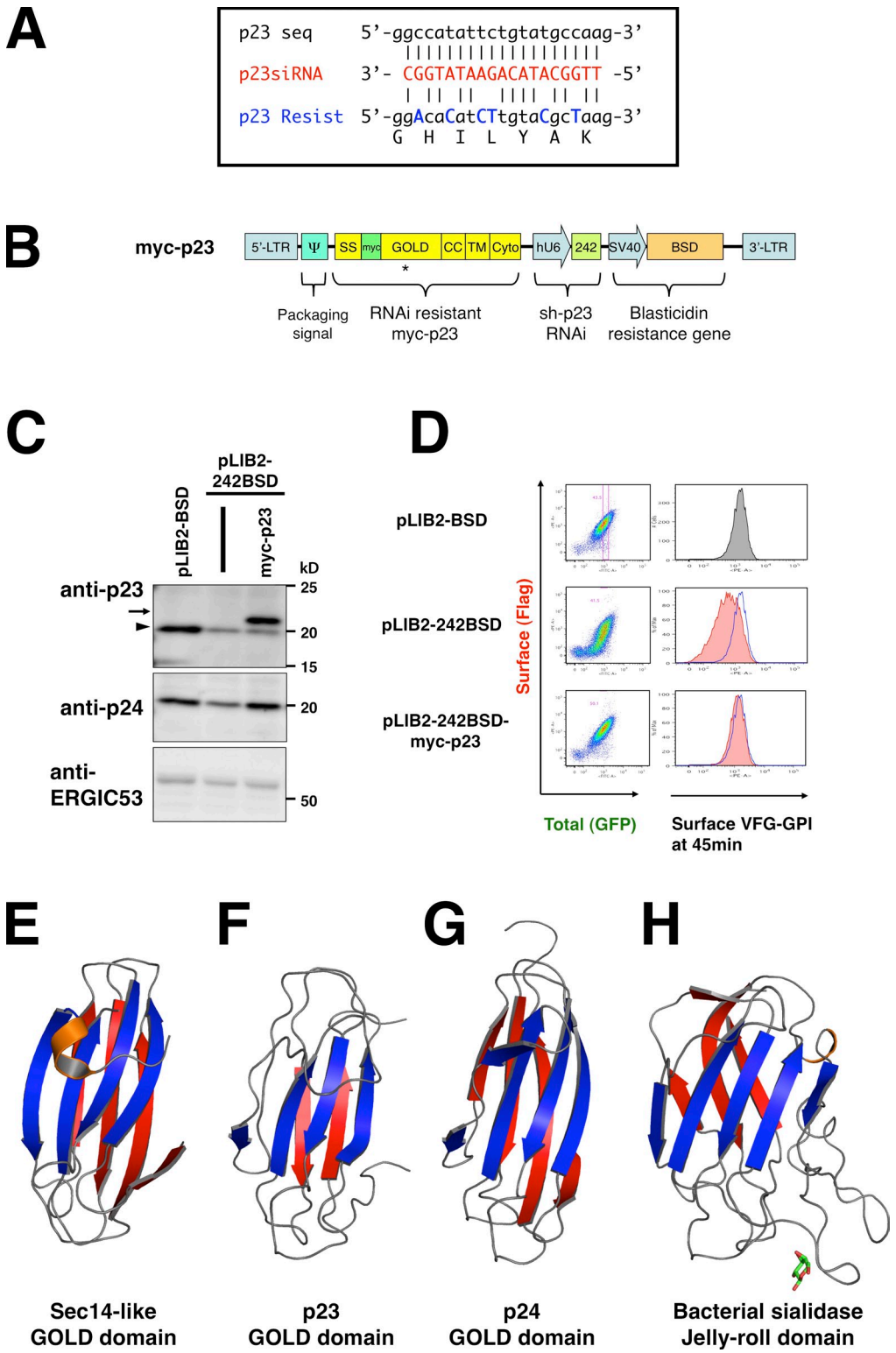

Figure S5. **Construction of myc-tagged p23 and modeling of p23 and p24.** (A) Sequence of RNAi-resistant p23. The p23 sequence in golden hamster (p23 seq), knockdown sequence of p23 (p23siRNA), and RNAi-resistant construct of p23 (p23 Resist) are shown in black, red, and blue, respectively. Replaced nucleotides in p23 Resist are shown in blue capital letters. Bottom, amino acid sequence. (B) Schematic representation of myc-tagged p23 construct. *, site of RNAi resistant sequence. (C) Western blotting of p23 and p24. FF8 cells stably transfected with an empty retrovirus vector (pLIB2-BSD), a vector containing the p23 siRNA construct (pLIB2-242BSD–), or vector shown in B (pLIB2-242BSD myc-p23) were established by infection with a retrovirus, followed by selection with 6 μg/ml blasticidin. The cells were lysed and the proteins were resolved by SDS-PAGE, followed by immunoblotting using a rabbit anti-p23, anti-p24, or anti-ERGIC53 antibody. Arrow, myc-p23; arrowhead, endogenous p23. (D) Flow cytometric analysis of VFG-GPI transport to the cell surface at 45 min after a temperature shift from 40°C to 32°C in FF8 cells stably transfected with pLIB2-BSD, pLIB2-242BSD, or pLIB2-242BSD myc-p23. The cell surface expression of VFG-GPI was analyzed by flow cytometry and shown as dot plots (left) and histograms (right). Blue lines in middle and bottom panels of histograms indicate the level of FF8 + pLIB2-BSD. (E–H) Homology models of p23–p24 GOLD domain. (E) Crystal structure of Sec14-like protein 2 GOLD domain (PDB accession no. 1O6U). (F) Homology model of p23 GOLD domain. (G) Homology model of p24 GOLD domain. (H) Crystal structure of jelly-roll domain of bacterial sialidase (PDB accession no. 1EUU) described by Gaskell et al. (1995). Bound galactose residue is shown as stick representation.

Reference

Gaskell, A., S. Crennell, and G. Taylor. 1995. The three domains of a bacterial sialidase: a beta-propeller, an immunoglobulin module and a galactose-binding jelly-roll. *Structure*. 3:1197–1205. doi:10.1016/S0969-2126(01)00255-6